IMPROVEMENT OF STATIC THRUST ESTIMATION

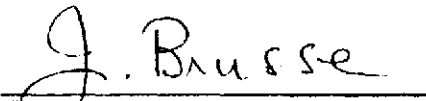BY J. Brusse and C. F. Kettleborough
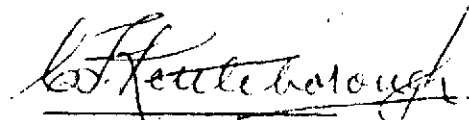
Final Report

to

National Aeronautics and Space Administration

Improvement of Propeller Static Thrust Estimation

NASA Research Grant No. NGR-44-001-011

Prepared by

J. Brusse
Engineering Research Associate

C.F. Kettleborough
Research Engineer

May 1975

Submitted by

Texas Engineering Experiment Station
Texas A&M University
College Station
Texas

ABSTRACT

This final report describes the aims of this research and the experimental
equipment set up at the Research Annex of Texas A&M University. A review
of theoretical considerations is presented together with a summary of the attempts
made to obtain a numerical solution and the difficulties encountered.

The final section of this report describes new work concerned with the
experimental determination of the chordwise pressure distribution during
operation at a tip speed of 500 ft/sec. Chordwise integration of the pressures
leads to the spanwise load distribution and further integration would give the
axial thrust.

INTRODUCTION

The work reported here has been carried out under NASA Grant NSG 669 initiated under the direction of Messrs. A. E. Cronk and J. C. Brusse. In submitting the renewal proposal in February 1967 , the investigators were Messrs. A. E. Cronk, C. F. Kettleborough and J. C. Brusse. At the end of the year Prof. A. E. Cronk was no longer a member of the team.

The problem to be studied was that of improving the performance estimation of propellers operating in the heavily loaded static thrust condition. The design of aircraft propellers by analytical methods, using the classical propeller theory of Goldstein has not been completely successful, particularly when performance optimization for the static thrust condition is attempted. The origin of the deficiencies in the analytical method is not apparent and has caused considerable concern in the development of propellor driven V/STOL aircraft.

EXPERIMENTAL CONSIDERATIONS

In order to assess the Goldstein Theory as it applies to propellers operating in the static thrust condition, it was considered necessary to inaugurate an experimental investigation to evaluate the performance of propellers alone and then to attempt correlation of analytically developed performance data with the experimentally generated data. It was also considered necessary to acquire a more complete understanding of the actual airflow phenomena in the vicinity of the propeller in order that the basic assumptions involved in the existing analytical methods can be assessed. Critical evaluation of the several propeller performance analytical methods indicated that a better knowledge of the radial loading distribution as well as the inflow of air into the propeller was

required. Consequently it appeared necessary that the experimental apparatus permit measurement of the air-flow at the propeller plane of rotation and perhaps the actual measurement of the radial load distribution on the blade itself. It was felt that if the flow patterns in the real fluid are understood more completely, the development of an analytical method would be much more easily attained. The ultimate aim of the research was the development of an analytical method which will yield performance estimates that more nearly compare to the actual performance observed.

The program called for the construction of a propeller static thrust dynamometer which would be adequate for conducting propeller performance experiments as well as the airflow studies. In addition to the static thrust dynamometer, a program of study and development of analytical methods useful in the prediction of propeller performance was to be carried out.

A propeller static thrust dynamometer designed to minimize wake and inflow interference has been constructed in a large airplane hangar at the Texas A&M Research Annex. The size and configuration of the dynamometer was determined after careful consideration of the following desirable features:

1. Test propellers must be isolated to the greatest degree possible.

2. The dynamometer must be capable of operating model propellers large enough to permit evaluation of Reynolds' Number effect.

3. The facility should be installed inside a building to avoid the vagaries of the weather.

With these factors in mind a configuration was conceived wherein the propeller is mounted so that it rotates in a horizontal plane with the line of thrust acting vertically upward. The propeller is rotated by a vertical shaft which turns inside a 7.5 inch diameter tubular steel housing. The housing has four slanted legs welded to its lower end which are bolted to specially constructed reinforced concrete piers eleven feet deep in the earth. The propeller plane

of rotation is 20 feet above the floor of the hangar and 10 feet below the roof joists. The curved hangar roof provides about 15 feet of additional overhead space that contains the roof supporting trusses. The nearest walls are in excess of 40 feet from the propeller. While the desirable condition of testing in an infinitely large air space has not been totally realized, it is believed the installation approximates this condition within practical limits.

Preliminary calculations indicated that approximately 400 horse-power would be required to operate 5-foot diameter, 4-way, high activity factor propellers at tip speeds of 900 feet per second. In addition to providing these values of power and speed, the power source must be easily controllable through a wide speed range. In the interest of economy, internal combustion engines were chosen for the power source instead of an electric motor drive. Two 275-HP Chris Craft V-8 Marine engines are installed to drive the vertical shaft through a differential gear box. Couplings are installed at each engine output shaft to allow for installation misalignment and vibration isolation. An overrunning clutch is mounted between the differential gear box output shaft and the main drive shaft to provide protection for the propeller balance in the event of mechanical failure in either of the power trains or the gear box. A splined axial-slip coupling is provided between the upper end of the main drive shaft and NASA provided propeller shaft to allow for thermal expansion and contraction of the shafts. A NASA strain-gaged propeller balance is mounted upstream of the thrust bearing and a propeller hub adapter shaft and propeller are then mounted directly to the balance. The electric signals from the balance are routed through a slip ring assembly and thence through conduit to amplifiers and the read-out gages. A 60-tooth steel gear is mounted on the propeller shaft between the balance and the thrust bearing to provide impulses through a magnetic pickup to an electronic tachometer. A small control house was built to house the power controls and the data acquisition equipment.

The slipring assembly originally used for transmission of the propeller balance strain gage signals caused considerable trouble in the initial stages of operation. Brush wear seemed excessive and because of inadequate air blast scavenging, the displaced brush particles were deposited around the inner walls of the brush holding assembly. These deposites provided variable resistance circuits between adjacent brushes and resulted in large fluctuations and zero shifts in the strain gage bridge output circuits. Cleaning of the slipring assembly was required after about 5 hours of operation and because of the necessity to recalibrate the data acquisition system after each disassembly the down-time was at least three days.

A slipring assembly having adequate cooling and scavenging provisions was installed during the month of July 1965 and has operated satisfactorily and without attention since that time. Some zero-shift between the beginning and end of each test run continues to be manifested, especially during the first 10-15 minutes of operation while the slipring assembly is cold. It has been observed that if the dynamometer is run for 20 or 30 minutes prior to taking any data, the zero-shift is reduced to insignificant values. With careful calibration and adjustment of the bridge power supplies, it appears possible to generate data which is repeatable within 2% of the measured performance of the propeller for C_p greater than .025.

A typical performance test for 5 foot diameter propellers requires the determination of thrust and torque for a range of rotational speeds from an arbitrary low value of 1500 RPM to the maximum allowable for the propeller being tested in approximately 200 RPM increments. The blade is set at a predetermined blade angle for each test run, the usual practice is to vary the blade angle at the reference station from zero to 25 degrees in 2.5 degree increments. Various performance parameters are calculated from the basic values of thrust, torque and rotational speed for each condition and blade angle tested.

In order to provide visual evaluation of the airflow surrounding the
propeller, a smoke generator with appropriate nozzles has been developed. In
addition to the smoke generator, a slavestrobe unit was purchased which permits
a gas discharge flashtube to be synchronized at any desired propeller
speed. The usual flow visualization technique required the light to flash
once per revolution of the propeller. With the smoke generator discharging
a filament of smoke at a prescribed point while being illuminated by the
flashes of the slavestrobe, an observer is able to get an idea of the relative
airflow velocity at various points as well as the direction of airflow through
the propeller. In addition to visual observation of the airflow phenomenon,
photographs with 3,000 ASA Polaroid film have been made. These photographs
show the general inflow pattern of air into the propeller as well as the vortex
system that is formed in the wake of the propeller. The helical path of
the airflow in the propeller slip stream also is observable. Thus the intro-
duction of smoke at various points around the rotating propeller has provided
a three-dimensional evaluation of the flow phenomenon associated with the
propeller operating in the highly loaded static thrust condition.

THEORETICAL CONSIDERATIONS

For many years the theory developed by Goldstein[1] has provided a
reliable means of calculating propeller performance. Modified by experience
factors and empirical corrections, this theory has been used intensively in
the design of propellers, largely for climb and cruise conditions of operations.
Attempts to optimize propeller designs for static thrust operation have in-
dicated discrepancies between theoretical performance and actual performance
achieved when the Goldstein theory is applied. This research is directed to-
ward investigating these discrepancies and attempting to develop improved
methods of calculating propeller performance for static thrust condition.

Possible discrepancies between the mathematical model postulated in the Goldstein theory and the physical flow situation are apparent.

1. Some of the power put into the propeller is lost in generating the trailing vortex field of the propeller wake. The theory assumes, following Betz[2], that the load distribution on the propeller blade is such as to minimize this power loss for a given thrust. In the heavily loaded static thrust condition there is no assurance that such an optimum load distribution is achieved.

2. As stated by Goldstein, the theory is valid only for small values of the ratio of the displacement velocity of the assumed helical vortex sheet to the velocity of advance of the propeller. Since this ratio becomes infinite in the static thrust condition it appears to be overly optimistic to expect the theory to hold with good accuracy in this situation.

3. The assumption of the propeller wake being in the form of helical vortex sheets of uniform pitch will be violated in the region immediately downstream of the propeller. In this region, herein called the near wake, the flow is accelerating in the axial direction and hence, the pitch is increasing. The near wake will be dominant in determining the inflow velocity field associated with the trailing vorticity. In addition, the instability of the vortex sheet and the tendency to roll up into discrete vortices will affect the inflow.

The interdependence of the blade load distribution, the trailing vortex field and the inflow velocity field poses a difficult problem that may not be amenable to a direct analytic solution.

Two methods of calculating the inflow velocity fields were selected for use in this investigation. They are the method of Iwasaki[3] which is an ex-

tension of methods presented by Kucheman[4] and the method of Wu[5]. Both methods involve an initial knowledge of the blade loading and so lend themselves to iterative procedures. In the experimental part of this program, the velocity fields were measured.

In the approach used by Wu the propeller is regarded as an actuator disk, normal to a uniform steady flow of an incompressible, inviscid fluid, Referred to a cylindrical coordinate system (r,θ,Z) with the Z axis coincident with the axis of rotation, positive direction downstream, the fluid velocity components are (u,v,w) respectively in the radial, tangential and axial directions. Since the flow is steady and axisymmetric a stream function can be expressed as a function of r and z from which two of the fluid velocity components u and w can be determined as

$$u = -\frac{1}{r}\frac{\partial \psi}{\partial z} \quad ; \quad w = +\frac{1}{r}\frac{\partial \psi}{\partial r} \tag{1}$$

The tangential velocity component v, must be specified separately. Considerations of conservation of angular momentum of the fluid show that the product vr must be a function of ψ in the slipstream and zero elsewhere.

Writing the equations of motion of the fluid in terms of the stream function results in

$$vr = f(\psi) \quad \text{in the slipstream}$$
$$= 0 \text{ elsewhere} \tag{2}$$

$$\frac{\partial^{2}\psi}{\partial r^{2}} - \frac{1}{r}\frac{\partial \psi}{\partial r} + \frac{\partial^{2}\psi}{\partial z^{2}} = \left(\Omega r^{2} - vr\right)\frac{d}{d\psi}vr = \left(\Omega r^{2} - vr\right)\left[\frac{\psi_{r}\frac{\partial}{\partial r}vr_{(3)} + \psi_{z}\frac{\partial}{\partial z}vr}{\psi_{z}^{2} + v_{r}^{2}}\right]$$

where Ω is the constant angular velocity of the propeller.

This constitutes a set of non-linear, partial differential equations for ψ and v. Two difficulties arise in obtaining solutions to these equations; namely, the nonlinearity apparent in the terms of the right-hand side of (3) and the fact that the slipstream region is not known.

These equations can be written in dimensionless form normalizing on the radius R as the unit of length and the remote uniform velocity, W. Utilizing differential operators that apply in a linear fashion and a perturbation stream function, ψ, it is possible to express the stream function ψ in a non-linear integral equation with the domain of integration not defined.

Since the domain of integration is determinable from the stream function a method of successive approximations is suggested. The problem of existence and uniqueness of solutions so obtained is mentioned by Wu but not treated by him. In addition, in the numerical calculation procedures some problems of numerical instabilities and lack of convergence in the interative procedures have appeared.

The approach used in this study is to retain the equations developed in dimensionless form, normalizing on W, the remote velocity. Attempts were made to extrapolate to the static thrust condition of W=0, in order to facilitate the numerical calculation procedure which involves an initial assumption of a stream function corresponding to the free stream flow undisturbed by the actuator disk. For the static thrust condition this would reduce to the trivial case of W=0 at all points or ψ = constant, which will not provide the required starting point for the calculation.

A program for calculation of the velocity field was developed following exactly the calculations described by Wu. This is an iterative procedure. Wu states that the second iteration gives results that are in general sufficiently accurate. However, it was found that an instability developed in the

third iteration that casts doubts on the accuracy of the second iteration.
It is therefore obvious that the second iteration does not produce a stable
answer. To this date no numerical results have been published using Wu's
method. Because of the lack of convegence of Wu's method of calculation an
alternative approach was considered in which equation (3) was cast in the form.

$$\begin{bmatrix} \text{MATRIX} \\ \text{OF} \\ \text{COEFFICIENTS} \end{bmatrix} \{\psi\} = \left\{ \begin{array}{c} R_{H_S} \\ V_{E_{C_T}} \\ D_R \end{array} \right\} \tag{4}$$

To specify the problem it is necessary to define the manner in which v
varies in the slipstream. A simple form was originally defined as v=kr
(where k is an experimental constant). The coordinates were made non-linear so
that a large number of grid points were situated along the axis and near the
propeller plane.

Other forms of the induced tangential velocity v were considered; these
clude:

$$v = kr^n \sqrt{1 - \frac{r}{r_p}} \tag{5}$$

$$v = Ar^a (1-r)^\beta \tag{6}$$

$$v = A(r-r_c)^n (1-r)^m \tag{7}$$

However, the shape of the slipstream downstream of the propeller is not
known and no method was found that allowed the shape to be determined. It is
known that the angular momentum in the slipstream must remain constant.

Several models based on this principle of conservation of angular momentum
were tested as part of the overall numerical solution. In all cases the shape
of the slipstream varied each iteration and could not be stabilized. Another

method was to initially guess the shape of the slipstream and then check for
consistency of angular momentum at each section. A correction to the
slipstream diameter could then be estimated so that angular momentum would be
conserved. However, this approach did not converge. Inspite of all efforts
no method was found which satisfactorily calculated the slipstream shape down-
stream and upstream of the propellor.

REFERENCES

1. Goldstein, S. On the Vortex Theory of Screw Propellers. Proc. Royal Society. A 123, 1929.

2. Betz, A.: Gottinger Machr., pp. 193-213, 1919.

3. Iwasaki, M.: Diagrams for Use In Calculation of Induced Velocity by Propellers. Kyushu University, Reports of Research Institute for Applied Mechanics, Vol. VI, No. 23, 1958.

4. Kucheman, D. and Weber, J.: Aerodynamics of Propulsion. McGraw-Hill, 1953.

5. Wu, T.Y.: Flow Through a Heavily Loaded Actuator Disk. Schiffstechnik, Band 9, Heft 47, 1962.

DETERMINATION OF BLADELOAD DISTRIBUTION

Propeller Blades

Two propeller test blades were made in accordance with the geometry described in figure 1. The unusual blade thickness was dictated partly by the requirement for pneumatic tubing to be inlaid into the blade surfaces and partly because bending and torsional stiffness was considered important. Since it was planned to conduct the tests at relatively low tip speed to stay away from compressibility effects, the 10% blade tip thickness was not considered detrimental.

The blades were milled from solid 7075-T651 aluminum bar stock, both blades being copied from a master blade by use of a milling machine hydraulic tracing attachment. Construction of the master blade involved the development of a set of airfoil templates for each spanwise orifice station. Each template was then copied in the master blade stock by use of the milling machine tracer attachment. The designed twist distribution was machined into the master blade by rotating it about its spanwise axis (.50 chord) to the required angle for each station template. The spaces between the spanwise stations were rough milled for fast material removal and then hand filed to a smooth transition surface. The final master blade shape was achieved by alternatively filing and checking both chordwise and spanwise profiles with a recording profilometer until the finished blade was within .005 inches of the designed contour.

After tracer milling two test blades from the master blade, spanwise grooves one-sixteenth wide were milled into both the upper and lower surfaces to provide space for inlaying the pneumatic tubing. Figure 2 presents the locations and the tube numbering for each blade. The grooving operation required the development and manufacture of a spacial cutter depth-limiting device and a holding fixture that provided blade rotation about its spanwise axis while the milling operation was in progress.

A paste type epoxy adhesive was used to bond one-sixteenth inch diameter hard brass tubing into the machined grooves. The paste was also bridged over the exposed tubing and provided a filler in the groove for subsequent filing to the blade contour. The shank end of each brass tube was fitted with a length of flexible plastic tubing which was then routed through appropriate holes in both upper and lower surfaces and out the end of the blade shank through a hole drilled along the blade spanwise centerline. After careful leak testing, all holes and pockets were expoxied over with more of the paste epoxy which, upon achieving complete curing, was also filed to the finished blade contour.

All of the blade orifices were drilled into the brass tubing with a 0.015 inch drill. Brass chips from the drilling operation were blown out the tip end of each tube with compressed air through the flexible tubing end. A piece of 1/32 inch diameter piano wire was used to ream each tube to remove any burrs at the junction of the drilled orifices and the tube bores. Great care was taken with the orifices to assure clean, round holes with as near identical lips as possible.

After the blades were completed and polished, each one was weighed to determine its weight and center of gravity. Only minor weight adjustments were required to bring both blades to near identical weight and c.g. location. Figure 3 presents a sketch of a test blade showing schematically the tubing layout and orifices.

Propeller Hub

The blade shanks were mounted in a ground adjustable, 4-way hub machined from AISI 4340 steel alloy, heat treated to 125,000 psi tensile strength. It was designed for flange mounting to the short shaft of the TAMU propeller static thrust dynamometer. A three-inch bore was provided along the axis of the hub to house a scanivalve and the flexible tubing from the blade orifices. A fiberglass spinner was constructed to provide additional protected space for the hub-

mounted data acquisition electronic equipment.

Scanivalve and Associated Equipment

A model 48D3 Scanivalve with a specially modified stepping motor was used for scanning the blade orifices during the test runs. A mounting fixture was devised that positioned the Scanivalve axial centerline on the dynamometer shaft axis of rotation, resulting in the Scanivalve pressure transducer rotating about an axis normal to its diaphragm plane. Because of the symmetry of the transducer and the relatively slow rotational speed attained, the centrifugal loading in the transducer diaphragm plane was quite small. In use, there was no measurable error resulting from the rotating transducer.

Special electronic devices were added to the rotating data acquisition equipment in the hub to minimized the effects of unsteady DC voltage transmission across the slipring assembly. Power for the Scanivalve was routed from a DC power supply in the control house to the stator side of the slipring assembly mounted on the dynamometer short shaft. Figure 4 presents a cut-away sketch of the propellor hub assembly. A miniaturized transducer excitation sub-regulator was mounted in the hub spinner along with the transducer balance and calibration device. The output from the transducer was changed to a FM signal in a miniaturized sub-carrier oscillator also mounted in the spinner. The FM data signal was transmitted through the sliprings and back into the control house to a discriminator which changed it back into the original analog signal. A signal conditioner and amplifier were provided for the position encoding device associated with the Scanivalve. Figure 5 is a block diagram of the data acquisition equipment.

Data Acquisition and Redording

The flexible plastic tubing extending into the hub bore from each propeller blade shank was connected to the Scanivalve tubulations in accordance with the

tubing numbering scheme shown in Figure 2. Scanivalve tubulations 41 through 44 were used in the determination of the transducer reference pressure.

In operation the Scanivalve was always started from the "home" position and stepped through each tubulation position until a complete scan of the pressure tubes was finished. For each Scanivalve position three separate pieces of data were recorded: propeller speed in rpm, Scanivalve position digits and the transducer output as a signed voltage.

Propeller rpm was sensed by a Hewlet-Packard 55RA digital counter set to count for one second the pulses generated by a magnetic pickup operating near a 60-tooth gear that turned with the dynamometer shaft. The Scanivalve position was determined by a special counter/controller that counted the pulses furnished by the Scanivalve position encoder during each step. The pressure transducer discriminator output was measured by a HP2104C integrating digital voltmeter. All of these counting and measuring devices provided visual digital display and an encoded BCD output.

The HP2515A high speed digital output scanner is a programmable switching device providing options for controlling up to nine data sources and a data recording device. As used for this test, the three data sources sensing rpm, position, and pressure were connected to the scanner with appropriate cabling while a HP 562A paper tape digital printer was used as the recording device.

Testing

A typical test began with checking or resetting the propeller blade angles. Each blade is set with an inclinometer at the same azimuth position to assure that each blade has the same setting. All pressure orifices are taped over with one mil mylar tape except the spanwise station on each blade to be measured. The transducer was electrically zeroed and the calibration resistance

inserted to check the bridge circuitry. A pressure scan was performed with
the propeller stationary—all transducer values for all the orifices should
be identical and zero. Any reading shown to be different usually indicated
a scanivalve problem or an obstructed orifice or tube.

After the "zero check" the dynamometer was started and brought to a speed
between 1500 and 2000 rpm and allowed to run at that speed for 15 to 20 minutes
to bring all mechanical and electronic equipment to normal operation
temperature. Immediately after stopping the dynamometer, another "zero check"
scan was performed to determine if any partial obstruction existed in any
of the pneumatic equipment. If there was no indication of pneumatic obstruction
or blockage and the zero setting of the transducer remained constant the
dynamometer was started again, brought to the required test speed and a pressure
scan was made. Following completion of the scan, the dynamometer was stopped
and the mylar tape was removed from the next station to be tested and the last
tested station was blocked with tape. The dynamometer was then started again
and another pressure scan was made. Testing continued in this manner until all
spanwise stations on each blade had been measured.

Data Reduction

Pressure measurements were recorded by the pressure transducer at the
center of rotation of the hub assembly. Hence a correction must be applied to
account for centrifugal effects along the brass tubing leading to the pressure
search holes. The pressure gradient is given by

$$\frac{\partial p}{\partial r} = \frac{\rho}{g} \frac{v^2}{r} \qquad \text{where} \quad V = \omega r \qquad (8)$$

From the characteristic gas equation $p = \rho RT$

$$\rho = P/RT \qquad (9)$$

Substituting equation (9) into equation (8) and integrating

$$\log_e p = \left(\frac{\omega^2}{2g RT}\right) r^2 + K \tag{10}$$

When r=0, p=p_m=measured value of the pressure, hence $K = \log_e p_m$

Hence
$$P = P_m e^{\left(\frac{\omega^2}{2g RT}\right) r^2} \tag{11}$$

(ω=angular velocity in rads/sec; R=the characteristic gas constant in ft.1b/1b/°F

T=temperature in°R; g=gravitational constant, 32.2 ft/sec^2; r=radius in feet)

This pressure is perpendicular to the surface of the propellor. Also the measured pressure must be corrected by any initial pressure measured by scanivalve tubulations located along the axis of spin in the hub. Hence the pressure perpendicular to the axis of rotation is

$$P = \left(P_m - P_c\right) e^{\left(\frac{\omega^2}{2g RT}\right) r^2} \cos\theta$$

where p_c = pressure correction and θ is the local chord angle. The transducer calibration was determined to be 0.001225 volts per square foot of pressure. All results were measured with the propellor rotating at a tip speed of 500 ft/sec

RESULTS

Typical pressure distributions at chord positions given by r/R = 0.3, 0.5, 0.75 and 0.95 are shown in figures 6 and 7. Spanwise net load distributions are shown in figure 8 for $\beta_{0.75r}$ = 5, 10°and 15° This figure clearly demonstrates that the load distribution is a maximum near the tip radius and increases with the

$\beta_{0.75r}$ angle. Integration of figure 8 would give the total load.
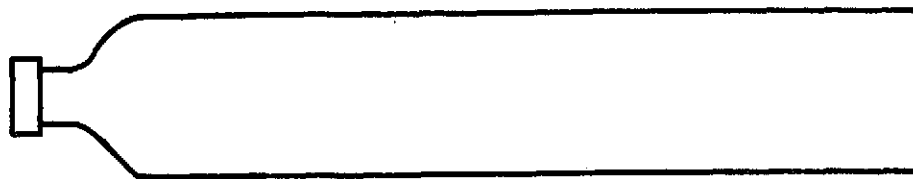
NACA 16 – 0XX
AF =   130
D   =   5 FT
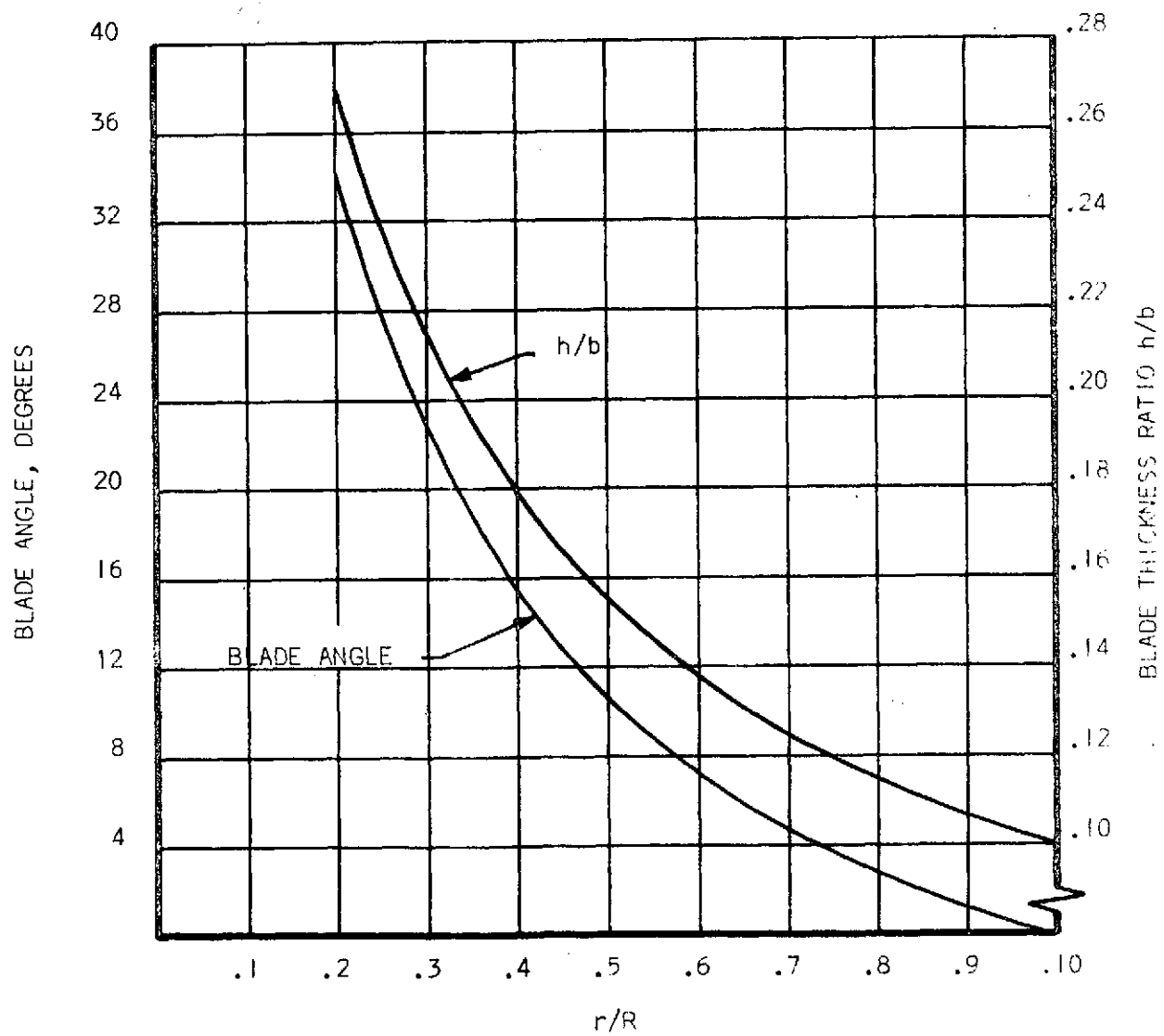
Figure 1. Propeller Blade Geometry

BLADE #1
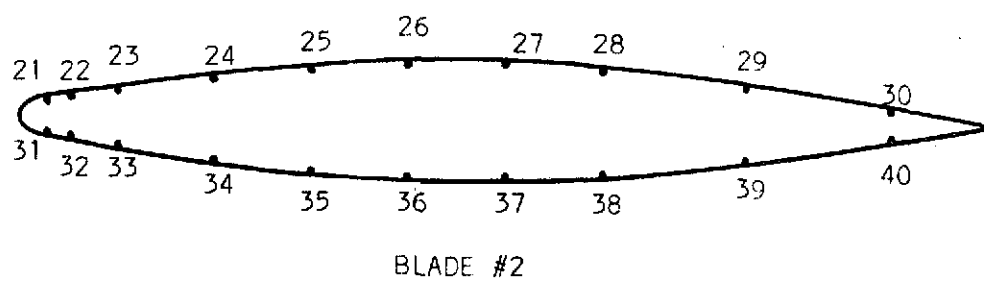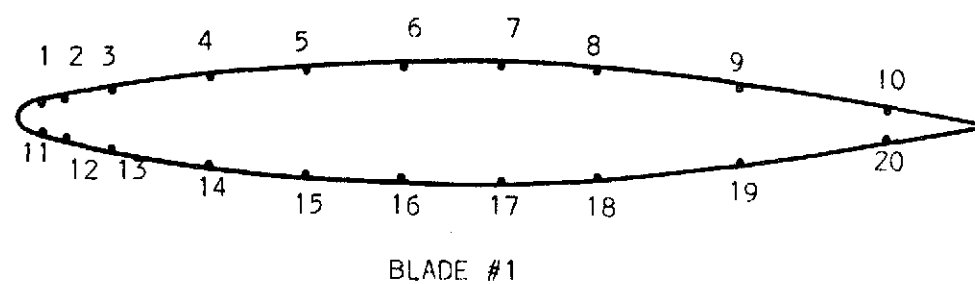
BLADE #2

x/C
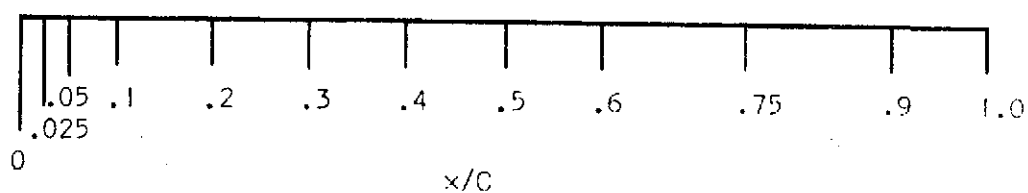
BLADE CROSS SECTION IS AT .6 r/R SPANWISE STATION

Figure 2.   Chordwise Location and Designation of Pneumatic Tubing

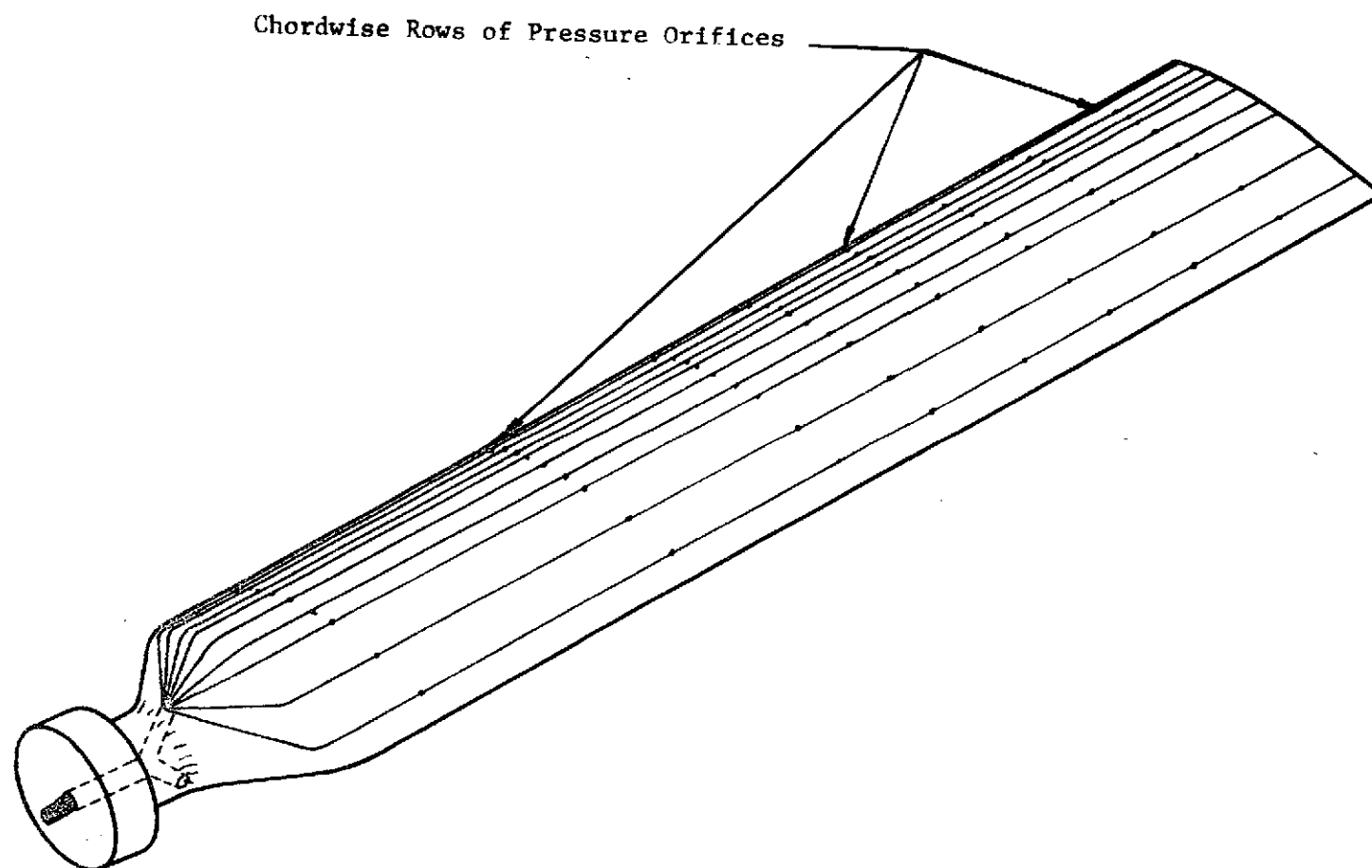Chordwise Rows of Pressure Orifices

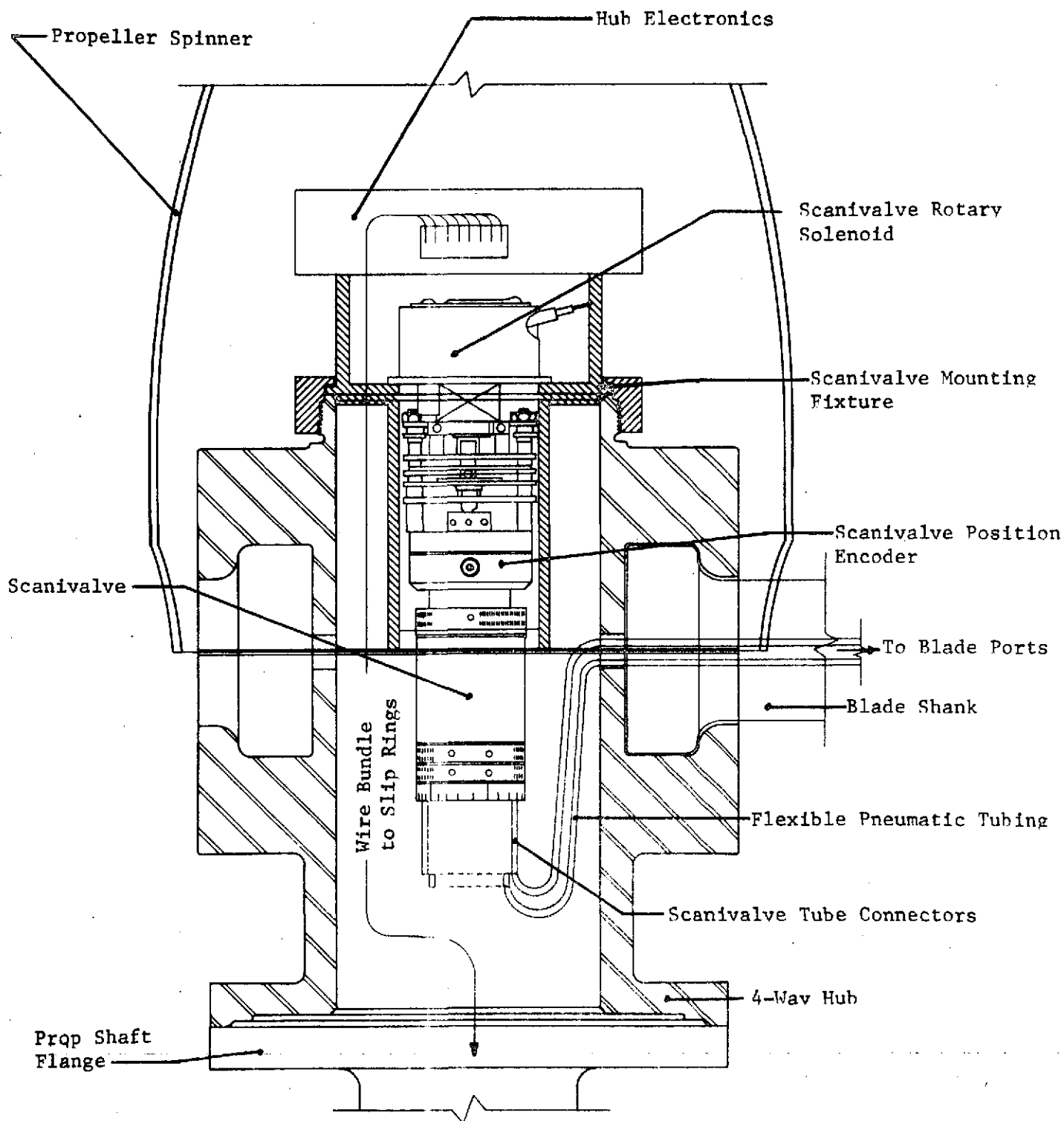Figure 3.   Test Blade With Holes Drilled

Figure 4.   Cut Away of Propeller Hub Assembly
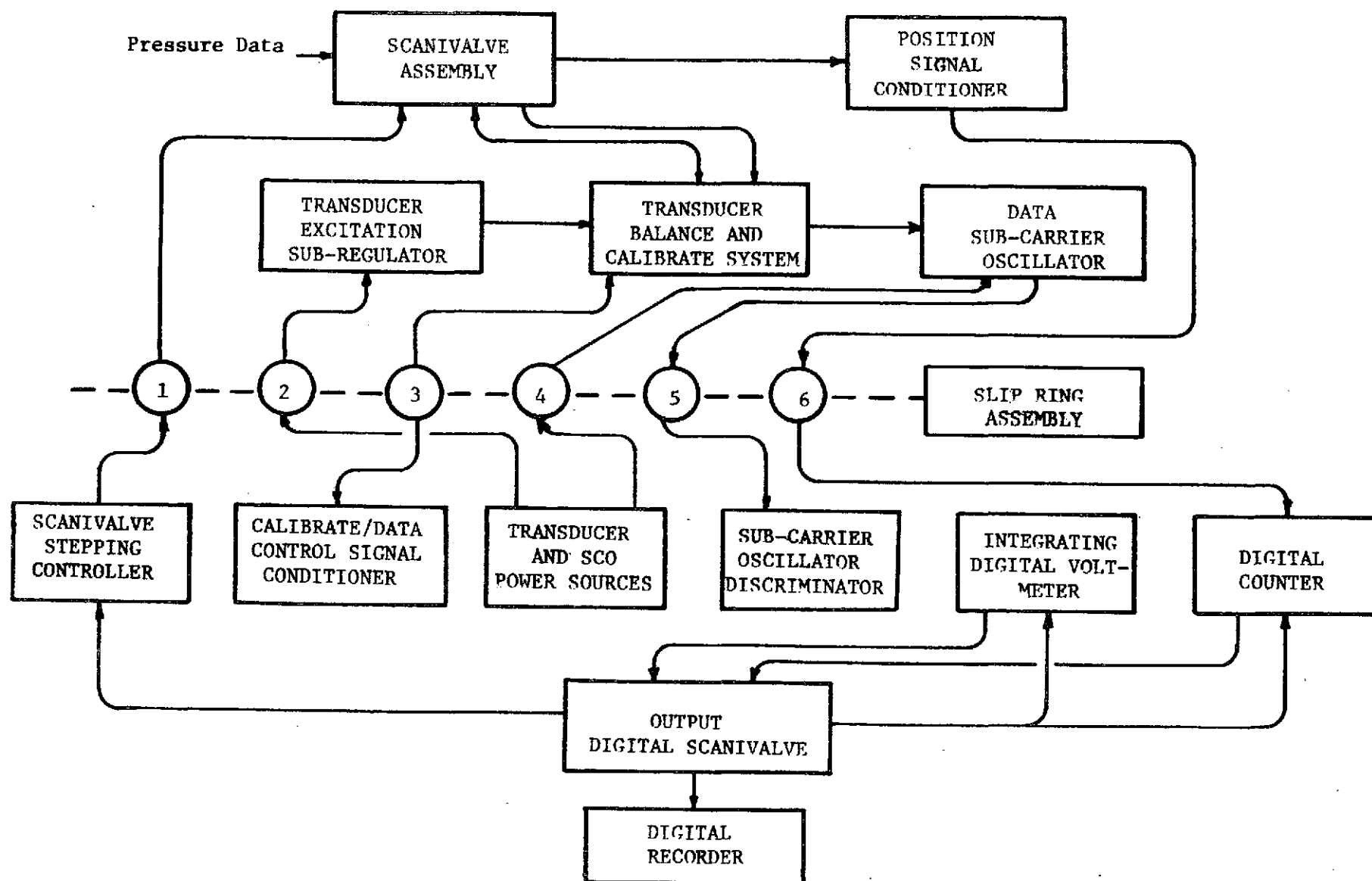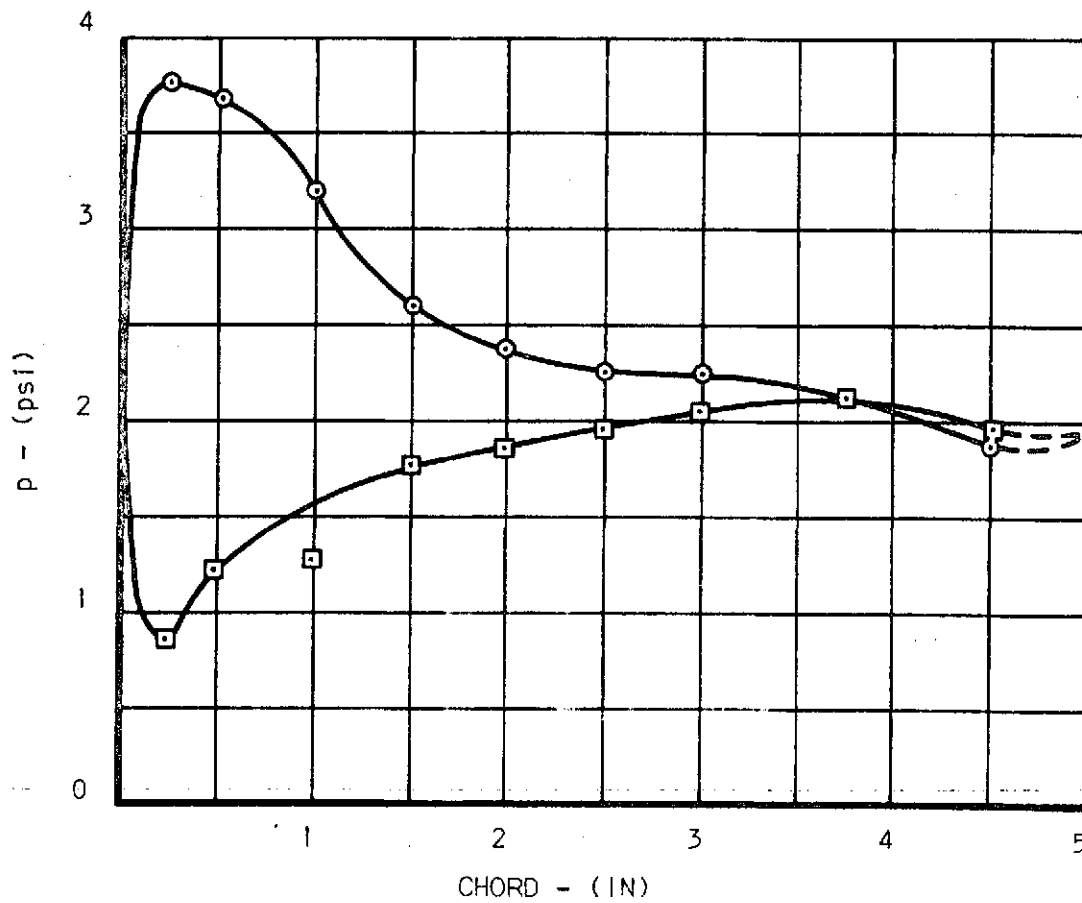
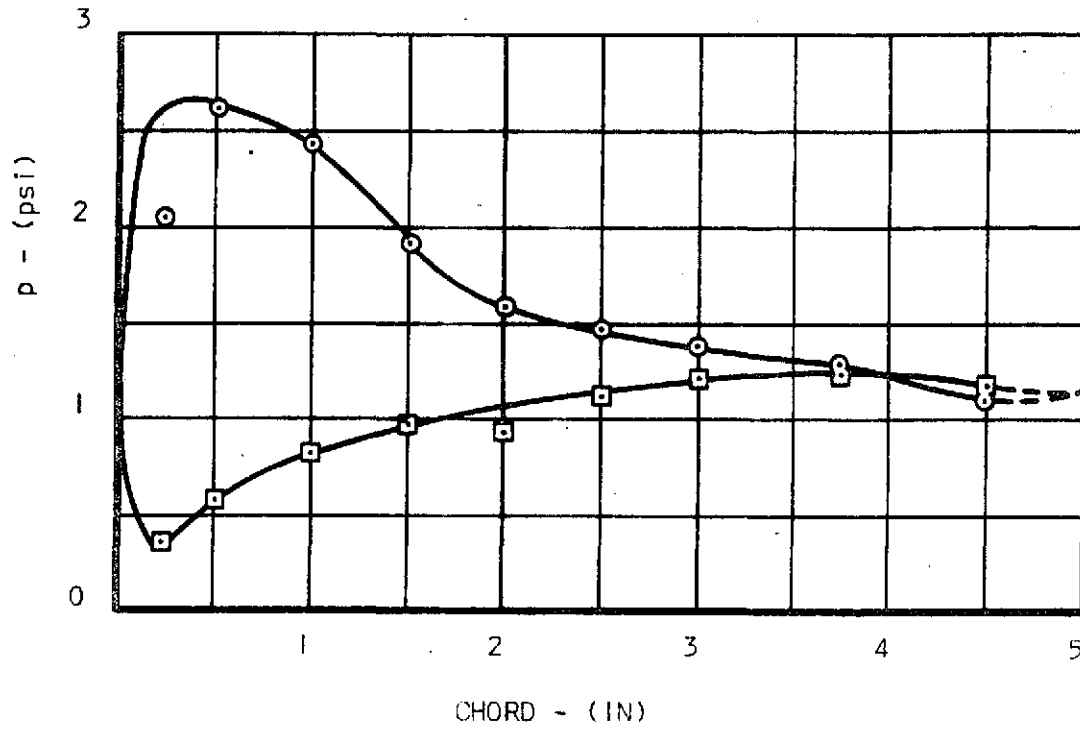Figure 5.   Data Acquisition Block Diagram

Figure 7.   Blade Pressure Data at $\beta_{.75} = 15^{\circ}$
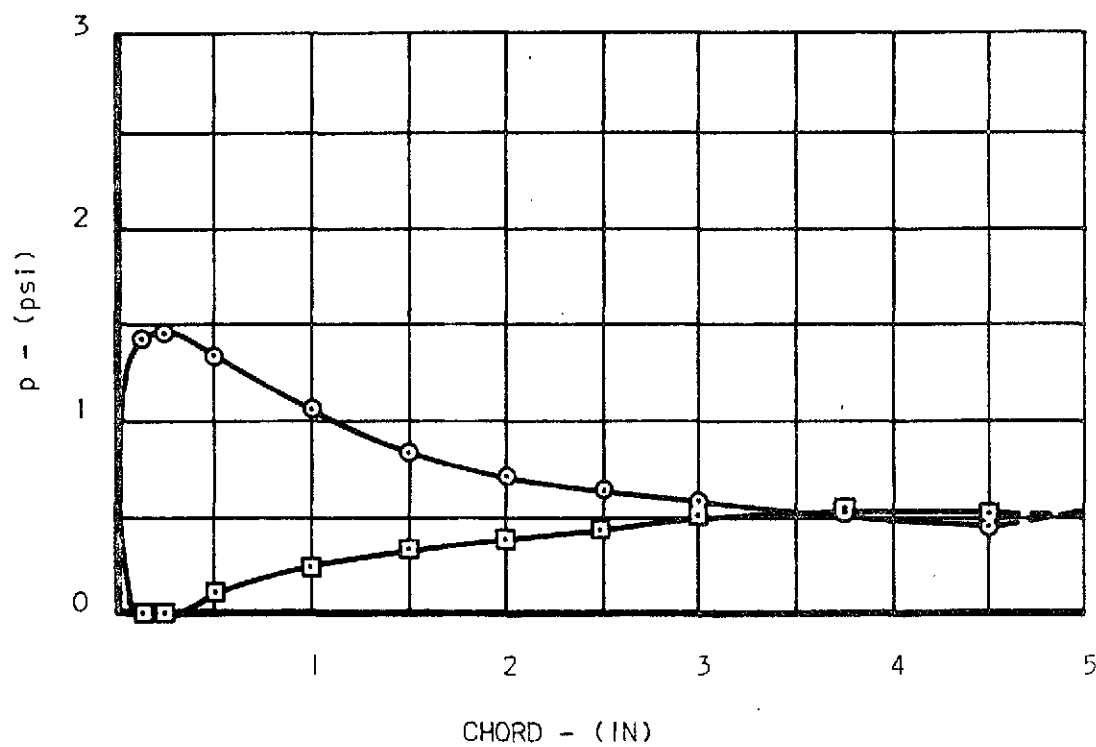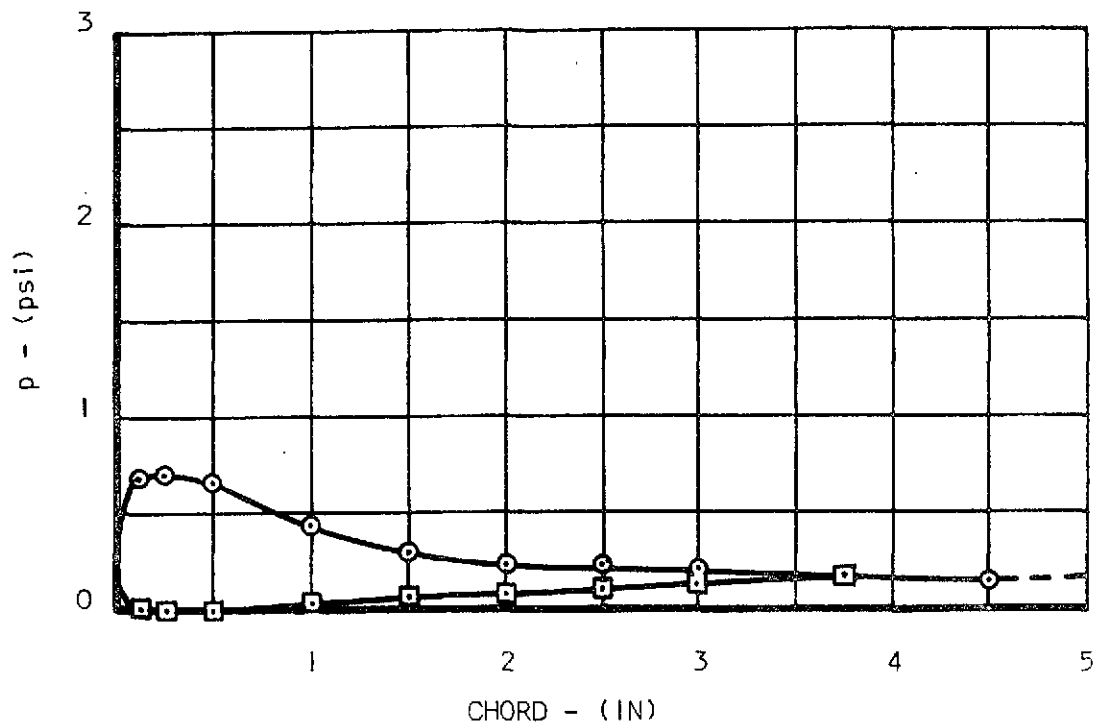for r/R = .75 (Top) and r/R = .95 (Bottom)

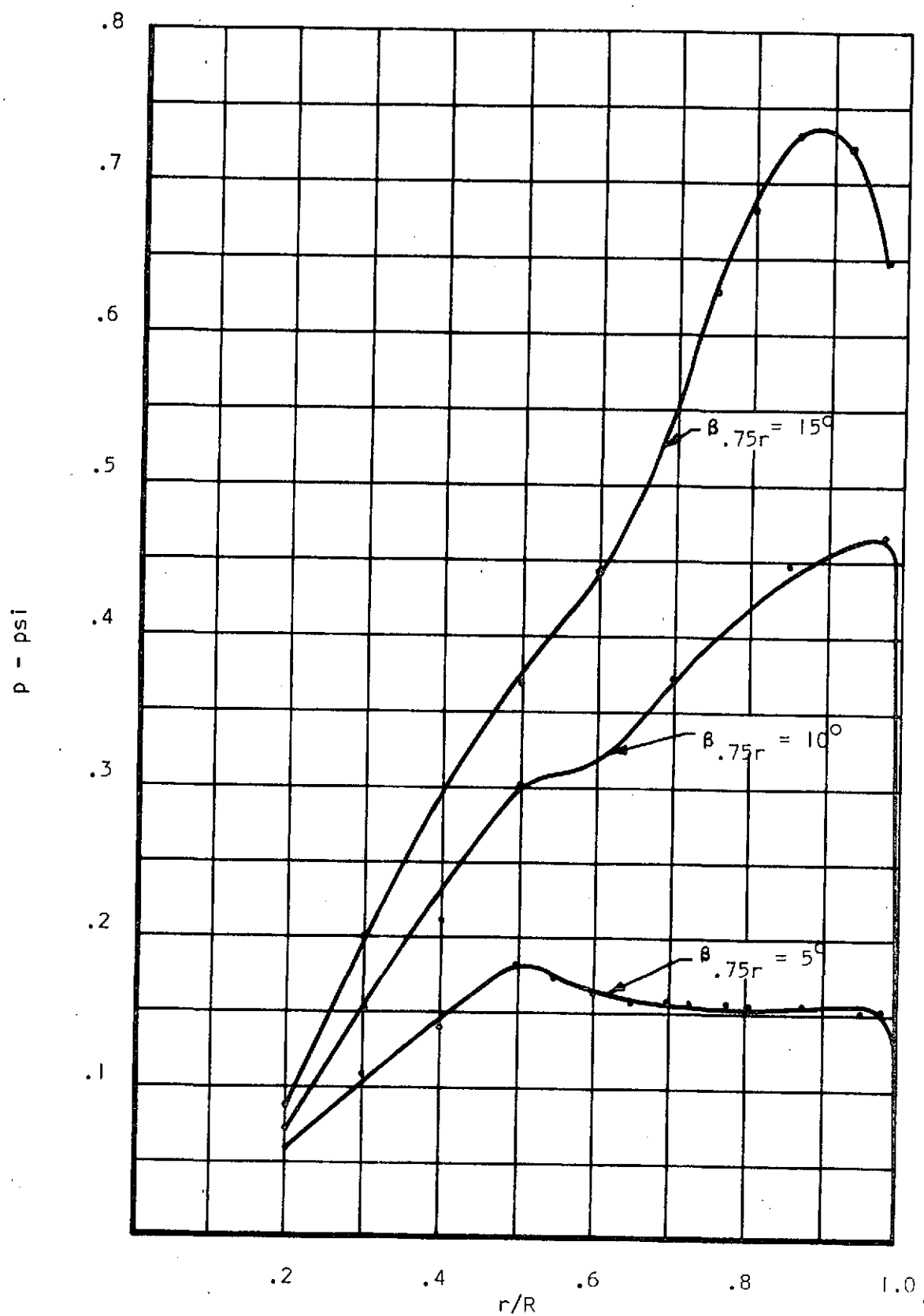Figure 6.   Blade Pressure Data at $\beta_{.75} = 15^{\circ}$
for r/R = .3 (Top) and r/R = .5 (Bottom)

Figure 8.   Spanwise Load Distribution